Accepted Manuscript

Synthesis of urea analogues bearing *N*-alkyl-*N*'-(thiophen-2-yl) scaffold and evaluation of their innate immune response to toll-like receptors

Zhipeng Chen, Xiaohong Cen, Junjie Yang, Zhiman Lin, Meihuan Liu, Kui Cheng

Synthesis of urea analogues bearing N-alkyl-N'-(thiophen-2-yl) scaffold and evaluation of their innate immune response to toll-like receptors

Zhipeng Chen†, Xiaohong Cen†, Junjie Yang†, Zhiman Lin, Meihuan Liu, Kui Cheng*

Guangdong Provincial Key Laboratory of New Drug Screening and Guangzhou Key Laboratory of Drug Research for Emerging Virus Prevention and Treatment, School of Pharmaceutical Sciences, Southern Medical University, Guangzhou, 510515, China.

Phone: +86 20 6164 7192, Fax: +86 20 6164 8533

Email address: Chengk@smu.edu.cn

†These authors contributed equally to this work.

Abstract:

Previous high throughput virtual screening of 10 million-compound and following cell based validation led to the discovery of a novel, nonlipopeptide-like chemotype ZINC 6662436, as toll-like receptor 2 (TLR2) agonists. In this report, compounds belonging to four areas of structural modification of ZINC6662436 were evaluated for biological activity using human HEK-Blue TLR2 reporter cells, and human THP-1 monocytic cells, yield SMU-C13 as an optimized, direct and high potent (EC_{50}=160 nM) agonist of human TLR2. Moreover, preliminary mechanism studies indicated that SMU-C13 through activates TLR1 and TLR2 then stimulates the NF-κB activation to trigger the downstream cytokines, such as TNF-α and secreted alkaline phosphatase (SEAP).

Keywords: Toll-like receptor 2 (TLR2); Small molecule antagonist; Inflammatory; Tumor immunity.

1. Introduction

Toll-like receptors (TLRs), which are expressed by various cells of the immune system, such as macrophages, dendritic cells and epithelial cells, can recognize and respond to molecules derived from bacterial, viral and fungal pathogens [1-5]. Generally, TLRs, particularly TLR2, are the major components of innate or adaptive immunity by recognizing conserved patterns in diverse microbial molecules, and TLR2 cooperation with TLR1 or TLR6 broads the range of recognition ligands [6-8]. In terms of function, recent evidence suggests that TLR2 is essential for sensing Gram-positive bacteria including peptidoglycans, lipoteichoic acid and bacterial lipoproteins. When activated, it can convey signals to transcription factors that can influence the nature of the adaptive T- or B-cell response [9-11]. Because TLRs specifically respond to the infection of microbial origin's products and direct the adaptive immune responses against antigens of microbial origin, just like other TLRs, TLR2 also has become a desirable target for vaccine adjuvants and cancer treatment in recent years. TLR2 agonists have been tested *in vitro* and *in vivo* for their ability to activate an antitumor immune response against several cancers [12-14]. The combination of TLR1/2 agonist (Diprovocim, EC_{50} 110 pM in THP-1 cells) and PD-L1 antibody showed great synergistic effect for tumor inhibition, and form long-term antitumor memory effect [15, 16].

These potential tumor immune effects have spurred our enthusiasm for discovering and developing new TLR2 selective agonists. While TLR2 recognizes a wide range of ligands, many of which are from Gram-positive bacteria, and it signals as a

heterodimer with either TLR1 or TLR6 [9], raising questions about the specificity of small molecule agents. Besides, until today, none of the TLR2 agonists in clinical or preclinical development are small molecules, and some contain mixtures with more than one active ingredient. Our group has focused on small molecules that target the TLR2 heterodimer protein-protein interaction [17, 18], specifically modulating the TLR1/2 response [19, 20].

Recently, 10 million-compound (10,519,614) from ZINC drug database was screened against the Pam_3CSK_4-binding domain of TLR1/2 (crystal structure PDB: 2Z7X) [9] using the Glide 7.4 program and yield compound ZINC6662436 as potent TLR2 small molecule agonist probe [21]. In the current study, we report the results of structure-activity relationship (SAR) study in ethyl 2-(4-methylpiperazine-1-carboxamido)-5,6-dihydro-4H-cyclopenta[b]thiophene-3-car boxylate scaffold with the goal of improving the potency of compound ZINC6662436. Four categories of modification of ZINC6662436 (SMU127) ring system were explored, while independently keeping all other structural features of the lead compound constant as depicted in **Figure 1**: (I) Changing the piperazine ring with bioisostere, such as piperidine, morpholine, or introducing different electron effect substitutions on the piperazine ring; (II) Modifications of the urea moiety with replacement of the oxygen by sulfur; (III) Modifications of the ethyl ester portion, including changing other alkyl groups, or replacing the ethyl group with carboxyl group; (IV) Ring enlargement derivatives in which the cyclopentyl ring portion was either replaced by cyclohexyl, substituted cyclohexyl, or cycloheptyl.

2. RESULTS AND DISCUSSION

2.1 Chemistry and SAR studies

The lead compound ZINC6662436 (SMU127) was synthesized from ethyl 2-isocyanato-5,6-dihydro-4*H*-cyclopenta[*b*]thiophene-3-carboxylate **A1** and 1-methylpiperazine **B1** as previously reported [21]. Moiety **A1** was obtained by mixture cyclopentanone, ethyl 2-cyanoacetate, sulfur and diethylamine at the sonicate condition following the Gewald procedure. To explore more SAR studies, moiety **C2-12** were synthesized in the similar conditions by using assorted of ketone and cyanoacetic ester (**Scheme 1**).

The synthesis of target analogues bearing substitution at the N^4-position of piperazine (**Figure 1**, I) was undertaken as follows. Intermediate **C1** reacts with bis(trichloromethyl)carbonate in dimethyl carbonate at 90 °C to afford compound **A1** without further purification, then *N*-substituted piperazine was added and stirred at room temperature to yield target compounds **3-5** (**Scheme 2**). Synthesis of piperidine or morpholine analogues was undertaken in similar reaction conditions only replacing the *N*-substituted piperazine with piperidine or morpholine (compounds **1** and **2**).

HEK-Blue hTLR2 cells were obtained by co-transfection of the human TLR2 and secreted embryonic alkaline phosphatase (SEAP) genes into HEK293 cells and were employed to test the compounds' TLR2 activities. As shown in **Table 1**, when piperizine was replaced by piperidine (**1**) or morpholine (**2**), the TLR2 activation activity was lost. The results suggested that piperizine scaffold was necessary for the

5

activity, next we performed a minor modification on the N^4 of piperizine position and investigated the substituent effects in the initial SAR study (**Figure 1**, part I). It was found that electro-donating substituents on piperizine group had very positive effect on TLR2 activity, while electro-withdraw substituents showed negative effect on the TLR2 activation (Table 1, compound **3**-**5**). The best substituent on N^4 of piperizine was methyl.

As the modification of position II (**Figure 1**), we replaced the oxygen with the electronic isostere sulfur together with different substituents on piperizine. The sulfur atom was generated from isothiocyanate (**F**) which obtained by reacting intermediates **C** with thiophosgen and triethylamine in dichloromethane at 0 °C. Next, isothiocyanates react with *N*-substituted piperazine to yield the target thiourea compounds (**Scheme 3**). The SAR studies showed that the agonist activity was decreased about 6 folds when oxygen atom replaced by sulfur atom (SMU127 vs **6**). As similar as the previous results, the TLR2 activity was disappeared when N^4 of piperizine was substituted by electro-withdraw group (**Table 1**, compounds **7**, **8**).

With these results in hand, we turn our attention to modify the third region (**Figure 1**, III) and keep 1-methyl piperizine substituent and oxygen constant. We introduced varying lengths of substituents from various aliphatic chains at the R_1 position. Compounds **9-11** were prepared by reacting 1-methyl piperazine with various **A** in similar reaction conditions (**Scheme 2**). Hydrolyzing compound **9** with LiOH in methanol/THF/H_2O solvent system provided the high yield hydrolyzed product **12**

(**Table 1**). The SAR for series **9-12** showed that methyl was the favorable substitution. The activity sequence was methyl > ethyl > isopropyl > propyl. When the number of carbon atoms was larger than 2 in the substitutions, the compounds showed less or no activities. The activity was disappeared when the ester was hydrolyzed to carboxyl group (**Table 1**, compound **12**).

The varied size of the ring has been studied in site IV (**Figure 1**, **Scheme 2**). It was found that six member ring fused[*b*]thiophene was the most favorable scaffold, and 5-membered rings caused 5 times reduction of activity (**13** vs SMU127). The activity of compound **14** was decreased 10 folds than that of compound **13** when the six member ring switched to seven. The size of substituent on 6-position of 4,5,6,7-tetrahydrobenzo[*b*]thiophene was also crucial for the activity and the activity decreased or disappeared with the size of substituents increasing (**Table 1**, compounds **15, 16**). To further investigate the SAR results, compounds **17-28** were synthesized (**Scheme 2**, **3**). When the substituent of N^4 atom of piperizine was replaced by phenyl or acetyl group, the activity disappeared (**Table 1**, compounds **20**, **22**, **24**). Thiourea compounds, the oxygen replaced with sulfur, showed less potency than that of urea (**Table 1**, compounds **17** vs **25**, **18** vs **26**). The methyl ester was proved to be the favorable substituent on R_1 position, and the activities of compounds **17** and **18** decreased 2 to 30 folds compared with compound **13** (SMU-C13). Over all, with four positions of SAR studies, we obtained compound SMU-C13 possessed the highest agonist TLR2 activity and was selected out for further evaluation.

7

2.2. Biological activity.

2.2.1 Specificity validation of SMU-C13.

As we know, the TLR family contains both intracellular and extracellular members. Here we selected the respective extracellular membrane protein (TLR4) and intracellular member (TLR3) to verify the specificity of SMU-C13. As shown in **Figure 2A**, the compound SMU-C13 can effectively active the TLR2 triggered SEAP signaling in HEK-Blue hTLR2 cells with no activation to the TLR4 and TLR3 signaling in other HEK-Blue hTLRs (**Fig. 2B**). The Poly IC and LPS used as positive controls which can significantly activate the signals of TLR4 and TLR3, respectively. The experiment results showed that SMU-C13 has very good specificity to TLR2. We also evaluated whether SMU-C13 binds to TLR2 on the cell surface and induces TLR2 expression in the whole-cell environment. HEK-Blue hTLR2 cells, which overexpress the human TLR2, were stimulated with SMU-C13. Cell lysates were subjected to immunoprecipitation and immuno-detected using TLR2 antibody. As shown in **Figure 2C**, with the dose of SMU-C13 increased, the expression of TLR2 was gradually increased. The TLR2 protein upregulated more than 5-fold when treated with 0.1 μM SMU-C13 vs the blank control, and the highest TLR2 expression level was achieved about 8-fold with the addition of 10 μM SMU-C13 (**Fig. 2D**). These results indicate that SMU-C13 is a specific agonist of TLR2 and is capable of binding to TLR2 on the cell surface to promote expression of TLR2 protein.

2.2.2 Antibody specificity studies.

8

TLR2 itself is unable to initiate an immune response, and it needs to form a dimerization with another protein, TLR1 or TLR6, in order to function normally. TLR1 and TLR6 are endogenously expressed in HEK-Blue hTLR2 cells, and whether SMU-C13 is an activator of TLR1/2 or an activator of TLR2/6 is unclear. Here we validate this result through antibodies experiments. When adding SMU-C13 to HEK-Blue hTLR2, we added different antibodies, including anti-TLR1, anti-TLR2 or anti-TLR6, to see which one or which TLRs were inhibited. The results showed that anti-TLR1 and anti-TLR2 antibodies had a very significant inhibition on the SEAP signal produced by SMU-C13, while anti-TLR6 antibody had no effect (**Fig. 3**). This experiment confirmed that SMU-C13 was an activator of TLR1/2 but not TLR2/6.

2.2.3 Downstream signaling evaluation.

Tumor necrosis factor α (TNF-α) is an important inflammatory cytokine produced after TLR2 promoted NF-κB activation, also one of the most active bioactive factors found to kill tumors so far. In this paper, the TNF-α was tested in phorbol 12-myristate 13-acetate (PMA)-differentiated human monocytic (THP-1) myeloid cells [15]. As show in **Figure 4A**, SMU-C13 induced dose-dependent TNF-α production after treat with the THP-1 cells for 4 hours. Meanwhile, SEAP assay data in human HEK-Blue TLR2 cells showed that SMU-C13 can strongly trigger the alkaline phosphatase secretion after NF-κB activation, and this activation can be suppressed by the classical NF-κB inhibitor triptolide (**Fig. 4B**). In summary, preliminary cytokine and protein levels studies have shown that SMU-C13 activates

TLR1/2, which initiates NF-κB signaling pathways to activate downstream signaling factors such as TNF and SEAP.

2.2.4 *In vitro* cytotoxicity studies

The toxicity of the compound was evaluated by a CCK8 colorimetric method. From the cell viability data (**Fig. 5**) we can confirm that SMU-C13 had no cytotoxicity as concentration up to 100 μM. Considering compound SMU-C13 having the highest TLR2 activation activity (EC_{50} =160±10 nM), low toxicity, as well as appropriate molecular weight, it might own the higher drug-like potential ability.

2.2.5 Molecular docking studies of SMU-C13.

The TLR1/2 agonist Pam3CSK4 binding to TLR1/TLR2 complex causes hetrodimerization of the extracellular domains to form a TLR1/TLR2/Pam3CSK4 complex, a human complex crystal structure which has been solved by Lee *et al* [9]. Previous experiments have demonstrated that SMU-C13 can trigger downstream cytokines, as well as directly active hTLR1 and hTLR2 protein directly in the antibody assay. To examine possible explanations for the significantly TLR1/2 activation potency in human cells, we explored the predicted binding mode(s) of compound SMU-C13 with the TLR1/TLR2 complex by conducting molecular docking experiments in the human protein crystal complex (PDB 2Z7X). We selected the most favorable energy configuration of SMU-C13 (shown in green) (**Fig. 6A**) and compared the binding of Pam3CSK4 (shown in red) bound to the complex (**Fig. 6B**).

Of particular interest is that SMU-C13 is well binding to the interface of TLR1 (purple) and TLR2 (yellow), tightly fit into the binding site of Pam3CSK4 and TLR1 and TLR2 (Fig. 6B), and shows significant interaction with the important residues, such as Gly313, Gln316 on TLR1 and Phe349 on TLR2 (**Fig. 6C**). The six-membered cyclohexane group and the methyl ester group are located on the moderately active pocket of the protein, which explains why enlarging the size of the ring or extending the ester chain results in a decrease in activity. Changes in N^4 position on the piperidine ring causing the interaction between the small molecule and the protein are influenced, so the activity is also varying. From the computer simulation, we can see that the small molecule well fit in the surface of dimer interface and greatly influence the potency of SMU-C13 in the TLR1/2 activity.

3. Conclusion

In this study, a series of ZINC 6662436 derivatives, were designed and synthesized, and their potential TLR2 activity was evaluated in HEK-Blue hTLR2 cells, and human THP-1 cells. The SAR results indicated that the piperidine ring, rather than the piperazine ring or the morpholine ring, contributes to the activity of TLR2; further studies have confirmed that the H at the N^4 piperidine ring is substituted with a methyl group as the optimal substituent. When the urea group in ZINC6662436 is substituted by thiourea, its activity almost completely disappears. Meanwhile, when the five-membered ring is expanded to a six-membered ring in the structure, the activity is increased, while the activity is decreased when the six-member ring switch

to seven. Considering the steric hindrance, electronegativity and electron effects of various substituent groups, we obtained an optimal compound SMU-C13 with EC_{50} at 160 ± 10 nM.

Following specificity assays in various HEK-Blue hTLRs indicated SMU-C13 only active TLR2 signaling with no influence to TLR3 and TLR4. Notably, SMU-C13 can also effectively up-regulate the TLR2 expression, up to 8 times. Antibodies experiments showed that SMU-C13 active TLR2 through its associate with TLR1, not TLR6. Elisa assays results indicated SMU-C13 could trigger the TNF-α expression after NF-κB activation, and the NF-κB activation can be suppressed by the NF-κB inhibitor triptolide. Computer simulation indicated SMU-C13 tightly fit into the binding site of Pam3CSK4 and TLR1/2, and form important small molecule-protein interactions. Taken together, our work enriched the situation of lacking of small-molecule of TLR1/2 agonist family, and primary in vitro assays explores the working mechanism of SMU-C13 and provides an novel molecule probe for potential therapeutic applications, including vaccine adjuvants development and tumor immunity therapies.

4. Experimental section

4.1. Chemistry

General procedure for synthesis of intermediate **C**

Compound **C** was synthesized following to the procedure of Gewald *et al.* [22], as already reported with some minor modifications [21]. The mixture of ketone **D** (1

mmol), alkyl cyanoacetate **E** (1.1 mmol), sulfur (1.1 mmol), and diethylamine (1.1 mmol) in ethanol/methanol (10 mL) was kept at room temperature in an ultrasonic cleaner for 1-3 hours. After completion of the reaction, the solvent was evaporated to dryness under reduced pressure. The crude product was purified by flash column chromatography on silica gel (petroleum ether/ethyl acetate elute) to provide the product **C**.

methyl 2-amino-5,6-dihydro-4*H*-cyclopenta[*b*]thiophene-3-carboxylate (**C2**)

Yield: 96%. ^{1}H NMR (400 MHz, CDCl$_3$) δ 5.89 (s, 2H), 3.80 (s, 3H), 2.80-2.85 (m, 2H), 2.71-2.76 (m, 2H), 2.91-2.36 (m, 2H). ^{13}C NMR (101 MHz, DMSO-*d*$_6$) δ 168.5, 165.5, 141.8, 119.5, 99.6, 50.7, 30.8, 28.8, 27.0. ESI-MS: m/z 198.1 ([M+H]$^{+}$).

propyl 2-amino-5,6-dihydro-4*H*-cyclopenta[*b*]thiophene-3-carboxylate (**C3**)

Yield: 90%. ^{1}H NMR (400 MHz, CDCl$_3$) δ 5.74 (s, 2H), 4.18 (t, J_1 = 6.4 Hz, J_2 = 12.8 Hz, 2H), 2.83-2.87 (m, 2H), 2.71-2.75 (m, 2H), 2.31-2.37 (m, 2H), 1.71-1.77 (m, 2H), 1.02 (t, J_1 = 7.2 Hz, J_2 = 14.4 Hz, 3H). ^{13}C NMR (101 MHz, CDCl$_3$) δ 166.8, 166.0, 142.5, 121.1, 102.5, 65.1, 30.9, 28.9, 27.2, 22.2, 10.8. ESI-MS: m/z 226.1 ([M+H]$^{+}$).

isopropyl 2-amino-5,6-dihydro-4*H*-cyclopenta[*b*]thiophene-3-carboxylate (**C4**)

Yield: 91%. ^{1}H NMR (400 MHz, CDCl$_3$) δ 5.77 (s, 2H), 5.12-5.18 (m, 1H), 5.82-5.86 (m, 2H), 2.72-2.75 (m, 2H), 2.31-2.36 (m, 2H), 1.32 (d, J = 6.4 Hz, 6H). ^{13}C NMR (101 MHz, CDCl$_3$) δ 166.4, 165.3, 142.6, 121.0, 102.9, 66.5, 30.8, 28.8, 27.1, 22.1.

ESI-MS: m/z 226.2 ([M+H]$^+$).

methyl 2-amino-4,5,6,7-tetrahydrobenzo[*b*]thiophene-3-carboxylate (**C5**)

Yield: 95%. ^{1}H NMR (400 MHz, CDCl$_3$) δ 5.97 (s, 2H), 3.80 (s, 3H), 2.69-2.72 (m, 2H), 2.50-2.53 (m, 2H), 1.75-1.79 (m, 4H). ^{13}C NMR (101 MHz, CDCl$_3$) δ 166.4, 162.0, 132.3, 117.4, 105.3, 50.5, 26.8, 24.5, 23.2, 22.7. ESI-MS: m/z 212.1 ([M+H]$^+$).

methyl 2-amino-5,6,7,8-tetrahydro-4*H*-cyclohepta[*b*]thiophene-3-carboxylate (**C6**)
Yield: 90%. ^{1}H NMR (400 MHz, CDCl$_3$) δ 5.51 (s, 2H), 3.83 (s, 3H), 2.96-2.99 (m, 2H), 2.58-2.61 (m, 2H), 1.82-1.85 (m, 2H), 1.61-1.68 (m, 4H). ^{13}C NMR (101 MHz, CDCl$_3$) δ 166.4, 160.2, 137.8, 121.2, 107.2, 50.7, 32.1, 28.6, 28.6, 27.8, 27.0. ESI-MS: m/z 226.1 ([M+H]$^+$).

ethyl 2-amino-4,5,6,7-tetrahydrobenzo[*b*]thiophene-3-carboxylate (**C7**)

Yield: 94%. ^{1}H NMR (400 MHz, CDCl$_3$) δ 5.96 (s, 2H), 4.28 (q, 2H), 2.71-2.74 (m, 2H), 2.51-2.54 (m, 2H), 1.75-1.81 (m, 4H), 1.35 (t, J_1 = 7.2 Hz, J_2 = 14.4 Hz, 3H). ^{13}C NMR (101 MHz, CDCl$_3$) δ 166.1, 162.0, 132.3, 117.4, 105.4, 59.3, 26.9, 24.5, 23.2, 22.8, 14.4. ESI-MS: m/z 226.1 ([M+H]$^+$).

propyl 2-amino-4,5,6,7-tetrahydrobenzo[*b*]thiophene-3-carboxylate (**C8**)

Yield: 91%. ^{1}H NMR (400 MHz, CDCl$_3$) δ 5.84 (s, 2H), 4.19 (t, J_1 = 6.4 Hz, J_2 = 12.8 Hz, 2H), 2.72-2.74 (m, 2H), 2.51-2.54 (m, 2H), 1.73-1.81 (m, 6H), 1.02 (t, J_1 = 7.2 Hz, J_2 = 14.4 Hz, 3H). ^{13}C NMR (101 MHz, CDCl$_3$) δ 166.3, 162.1, 132.3, 117.4, 105.5,

14

65.2, 27.0, 24.5, 23.3, 22.9, 22.2, 10.8. ESI-MS: m/z 240.1 ([M+H]$^+$).

isopropyl 2-amino-4,5,6,7-tetrahydrobenzo[*b*]thiophene-3-carboxylate (**C9**)

Yield: 90%. ^{1}H NMR (400 MHz, CDCl$_3$) δ 5.67 (s, 2H), 5.15-5.21 (m, 1H), 2.71-2.74 (m, 2H), 2.50-2.54 (m, 2H), 1.74-1.81 (m, 4H), 1.34 (d, *J* = 7.2 Hz, 6H). ^{13}C NMR (101 MHz, CDCl$_3$) δ 165.6, 162.1, 132.2, 117.2, 105.4, 66.5, 27.0, 24.5, 23.2, 22.9, 22.1. ESI-MS: m/z 240.2 ([M+H]$^+$).

isopropyl 2-amino-5,6,7,8-tetrahydro-4*H*-cyclohepta[*b*]thiophene-3-carboxylate (**C10**)

Yield: 89%. ^{1}H NMR (400 MHz, CDCl$_3$) δ 5.76 (s, 2H), 5.16-5.23 (m, 1H), 2.98-3.00 (m, 2H), 2.50-2.53 (m, 2H), 1.63-1.83 (m, 6H), 1.34 (d, *J* = 6.4 Hz, 6H). ^{13}C NMR (101 MHz, CDCl$_3$) δ 165.3, 160.0, 137.7, 120.7, 107.3, 66.7, 32.0, 30.3, 27.8, 26.7, 24.2, 22.0. ESI-MS: m/z 254.1 ([M+H]$^+$).

methyl 2-amino-6-methyl-4,5,6,7-tetrahydrobenzo[*b*]thiophene-3-carboxylate (**C11**)
Yield: 93%. ^{1}H NMR (400 MHz, CDCl$_3$) δ 5.96 (s, 2H), 3.80 (s, 3H), 2.84-2.90 (m, 1H), 2.55-2.59 (m, 2H), 2.11-2.18 (m, 1H), 1.81-1.89 (m, 2H), 1.33-1.38 (m, 1H), 1.06 (d, *J* = 6.4 Hz, 3H). ^{13}C NMR (101 MHz, CDCl$_3$) δ 166.5, 162.3, 131.9, 117.0, 105.1, 50.6, 32.6, 31.1, 29.5, 26.7, 21.5. ESI-MS: m/z 226.1 ([M+H]$^+$).

methyl 2-amino-6-pentyl-4,5,6,7-tetrahydrobenzo[*b*]thiophene-3-carboxylate (**C12**)
Yield: 90%. ^{1}H NMR (400 MHz, CDCl$_3$) δ 5.93 (s, 2H), 3.80 (s, 3H), 2.84-2.90 (m,

1H), 2.57-2.62 (m, 2H), 2.13-2.19 (m, 1H), 1.73-1.91 (m, 2H), 1.31-1.38 (m, 9H), 0.92 (t, J_1 = 6.4 Hz, J_2 = 12.8 Hz, 3H). ^{13}C NMR (101 MHz, CDCl$_3$) δ 166.5, 162.2, 132.2, 117.2, 105.2, 50.5, 36.0, 34.5, 32.1, 30.9, 29.3, 26.7, 22.7, 14.1. ESI-MS: m/z 282.1 ([M+H]$^+$).

General procedure for synthesis of urea compounds (compounds **1-5**, **9-20**)

The mixture of intermediate **C** (1 mmol) and triphosgene (0.35 mmol) in dimethyl carbonate was kept at 90°C for 8h. After completion of the reaction, without further purification, substituted piperizine **B** (1.1 mmol) was added and stirred at room temperature [21]. After completion of the reaction, the solvent was evaporated to dryness under reduced pressure. The crude product was purified by flash column chromatography on silica gel (petroleum ether/ethyl acetate elute) to provide the urea product.

General procedure for synthesis of thiourea compounds (compounds **6-8**, **21-28**)

The mixture of **C** (1 mmol) and triethylamine (1.1 mmol) in dichloromethane was stirred at 0 °C. Thiophosgen (1.5 mmol) was dropped into the mixture to keep the temperature lower than 5 °C. After completion of the reaction, the solvent was evaporated to dryness under reduced pressure. Then, 50 mL dichloromethane was added and washed with water (5 mL) 2 times [23]. The solvent was dried with magnesium sulfate and evaporated to 10 mL, then substituted piperizine **B** (1.1 mmol) was added and stirred at room temperature. After completion of the reaction, the solvent was evaporated to dryness under reduced pressure. The crude product was

16

purified by flash column chromatography on silica gel (petroleum ether/ethyl acetate

elute) to provide the thiourea product.

ethyl

2-(piperidine-1-carboxamido)-5,6-dihydro-4*H*-cyclopenta[*b*]thiophene-3-carboxylate

(**1**)

Yield: 82%. ^{1}H NMR (400 MHz, CDCl$_3$) δ 10.78 (s, 1H), 4.31 (q, 2H), 3.52-3.53 (m,

4H), 2.81-2.88 (m, 4H), 2.36-2.38 (m, 2H), 1.66 (s, 6H), 1.37 (t, J_1 = 6.4 Hz, J_2 = 12.8

Hz, 3H). ^{13}C NMR (101 MHz, CDCl$_3$) δ 166.3, 155.6, 152.4, 140.5, 129.6, 105.4,

59.8, 44.7, 30.1, 28.6, 27.5, 25.4, 24.1, 14.0. HRMS (ESI): calcd for C$_{16}$H$_{22}$N$_2$O$_3$S

(M+H)$^+$ = 323.1429, found 323.1433.

ethyl

2-(morpholine-4-carboxamido)-5,6-dihydro-4*H*-cyclopenta[*b*]thiophene-3-carboxylat

e (**2**)

Yield: 85%. ^{1}H NMR (400 MHz, CDCl$_3$) δ 10.85 (s, 1H), 4.30 (q, 2H), 3.76-3.78 (m,

4H), 3.54-3.57 (m, 4H), 2.82-2.91 (m, 4H), 2.36-2.39 (m, 2H), 1.38 (t, J_1 = 7.2 Hz, J_2

= 14.4 Hz, 3H). ^{13}C NMR (101 MHz, CDCl$_3$) δ 166.4, 155.0, 152.7, 140.6, 130.0,

105.8, 66.1, 60.0, 43.7, 30.1, 28.6, 275, 14.1. HRMS (ESI): calcd for C$_{15}$H$_{20}$N$_2$O$_4$S

(M+H)$^+$ = 325.1222, found 325.1226.

ethyl

2-(4-ethylpiperazine-1-carboxamido)-5,6-dihydro-4*H*-cyclopenta[*b*]thiophene-3-carb

oxylate (**3**)

Yield: 90%. ^{1}H NMR (400 MHz, CDCl$_3$) δ 10.82 (s, 1H), 4.30 (q, 2H), 3.59-3.61 (m,

4H), 2.81-2.90 (m, 4H), 2.35-2.53 (m, 8H), 1.37 (t, J_1 = 7.2 Hz, J_2 = 14.4 Hz, 3H),

1.12 (t, J_1 = 7.2 Hz, J_2 = 14.4 Hz, 3H). ^{13}C NMR (101 MHz, CDCl$_3$) δ 166.5, 155.3,

152.5, 140.6, 129.9, 105.7, 59.9, 52.0, 52.0, 43.6, 30.2, 28.6, 27.5, 14.4, 11.7. HRMS

(ESI): calcd for C$_{17}$H$_{25}$N$_3$O$_3$S (M+H)$^+$ = 352.1695, found 352.1699.

ethyl

2-(4-(2-hydroxyethyl)piperazine-1-carboxamido)-5,6-dihydro-4*H*-cyclopenta[*b*]thiop

hene-3-carboxylate (**4**)

Yield: 80%. ^{1}H NMR (400 MHz, CDCl$_3$) δ 10.84 (s, 1H), 4.30 (q, 2H), 359-3.68 (m,

6H), 2.81-2.90 (m, 4H), 2.59-2.63 (m, 7H), 2.35-2.38 (m, 2H), 1.37 (t, J_1 = 7.2 Hz, J_2

= 14.4 Hz, 3H). ^{13}C NMR (101 MHz, CDCl$_3$) δ 166.6, 155.2, 152.7, 140.7, 130.1,

106.0, 60.1, 59.5, 58.0, 525, 43.6, 30.2, 28.7, 27.6, 14.2. HRMS (ESI): calcd for

C$_{17}$H$_{25}$N$_3$O$_4$S (M+H)$^+$ = 368.1644, found 368.1648.

ethyl

2-(4-acetylpiperazine-1-carboxamido)-5,6-dihydro-4*H*-cyclopenta[*b*]thiophene-3-carb

oxylate (**5**)

Yield: 86%. ^{1}H NMR (400 MHz, CDCl$_3$) δ 10.75 (s, 1H), 4.18-4.19 (m, 2H),

3.45-3.62 (m, 8H), 2.71-2.77 (m, 4H), 2.25-2.27 (m, 2H), 2.05 (s, 3H), 1.27 (t, J_1 =

7.2 Hz, J_2 = 14.4 Hz, 3H). ^{13}C NMR (101 MHz, CDCl$_3$) δ 168.9, 166.2, 154.6, 152.3, 140.6, 129.9, 105.9, 60.0, 45.4, 43.1, 40.4, 30.0, 28.5, 27.4, 21.0, 14.0. HRMS (ESI): calcd for C$_{17}$H$_{23}$N$_3$O$_4$S (M+H)$^+$ = 366.1488, found 366.1492.

ethyl

2-(4-methylpiperazine-1-carbothioamido)-5,6-dihydro-4*H*-cyclopenta[*b*]thiophene-3-carboxylate (**6**)

Yield: 91%. ^{1}H NMR (400 MHz, CDCl$_3$) δ 12.11 (s, 1H), 4.33 (q, 2H), 4.12 (s, 4H), 2.82-2.93 (m, 4H), 2.68 (s, 4H), 2.45 (s, 3H), 2.35-2.39 (m, 2H), 1.38 (t, J_1 = 7.2 Hz, J_2 = 14.4 Hz, 3H). ^{13}C NMR (101 MHz, CDCl$_3$) δ 175.7, 167.1, 155.8, 140.7, 131.4, 108.3, 60.5, 54.3, 47.6, 45.6, 30.4, 28.8, 27.6, 14.2. HRMS (ESI): calcd for C$_{16}$H$_{23}$N$_3$O$_2$S$_2$ (M+H)$^+$ = 354.1310, found 354.1315.

ethyl

2-(4-acetylpiperazine-1-carbothioamido)-5,6-dihydro-4*H*-cyclopenta[*b*]thiophene-3-c

arboxylate (**7**)

Yield: 88%. ^{1}H NMR (400 MHz, CDCl$_3$) δ 12.12 (s, 1H), 4.32 (q, 2H), 4.14-4.15 (m, 2H), 3.99-4.01 (m, 2H), 3.81-3.84 (m, 2H), 3.66-3.69 (m, 2H), 2.82-2.93 (m, 4H), 2.35-2.39 (m, 2H), 2.15 (s, 3H), 1.38 (t, J_1 = 7.2 Hz, J_2 = 14.4 Hz, 3H). ^{13}C NMR (101 MHz, CDCl$_3$) δ 176.3, 139.2, 166.7, 155.1, 140.6, 131.1, 108.2, 60.4, 46.7, 44.8, 40.0, 30.2, 28.7, 27.4, 21.2, 14.1. HRMS (ESI): calcd for C$_{17}$H$_{23}$N$_3$O$_3$S$_2$ (M+H)$^+$ = 382.1259, found 382.1263.

ethyl

2-(4-phenylpiperazine-1-carbothioamido)-5,6-dihydro-4*H*-cyclopenta[*b*]thiophene-3-

carboxylate (**8**)

Yield: 83%. ^{1}H NMR (400 MHz, CDCl$_3$) δ 12.14 (s, 1H), 7.31-7.34 (m, 2H),

6.94-6.98 (m, 3H), 4.32-4.37 (m, 2H), 4.20-4.23 (m, 4H), 3.39-3.41 (m, 4H),

2.84-2.95 (m, 4H), 2.36-2.40 (m, 2H), 1.40 (t, J_1 = 7.2 Hz, J_2 = 14.4 Hz, 3H). ^{13}C

NMR (101 MHz, CDCl$_3$) δ 175.8, 167.2, 155.9, 150.2, 140.8, 131.6, 129.3, 120.1,

115.9, 108.4, 60.6, 48.3, 47.5, 30.5, 28.9, 27.7, 14.3. HRMS (ESI): calcd for

C$_{21}$H$_{25}$N$_3$O$_2$S$_2$ (M+H)$^+$ = 416.1466, found 416.1471.

methyl

2-(4-methylpiperazine-1-carboxamido)-5,6-dihydro-4*H*-cyclopenta[*b*]thiophene-3-car

boxylate (**9**)

Yield: 92%. ^{1}H NMR (400 MHz, CDCl$_3$) δ 10.81 (s, 1H), 3.85 (s, 3H), 3.57-3.60 (m,

4H), 2.82-2.84 (m, 4H), 2.46-2.49 (m, 4H), 2.34-2.36 (m, 5H). ^{13}C NMR (101 MHz,

CDCl$_3$) δ 166.8, 155.4, 152.4, 140.4, 129.9, 105.4, 54.3, 51.1, 45.8, 43.4, 30.0, 28.6,

27.5. HRMS (ESI): calcd for C$_{15}$H$_{21}$N$_3$O$_3$S (M+H)$^+$ = 324.1382, found 324.1386.

propyl

2-(4-methylpiperazine-1-carboxamido)-5,6-dihydro-4*H*-cyclopenta[*b*]thiophene-3-car

boxylate (**10**)

Yield: 81%. ^{1}H NMR (400 MHz, CDCl$_3$) δ 10.86 (s, 1H), 4.22 (t, J_1 = 6.4 Hz, J_2 =

12.8 Hz, 2H), 3.58-3.62 (m, 4H), 2.82-2.92 (m, 4H), 2.47-2.52 (m, 4H), 2.35-2.40 (m, 5H), 1.75-1.80 (m, 2H), 1.04 (t, J_1 = 7.2 Hz, J_2 = 14.4 Hz, 3H). ^{13}C NMR (101 MHz, CDCl$_3$) δ 166.8, 155.5, 152.7, 140.7, 130.1, 105.9, 65.8, 54.4, 45.9, 43.6, 30.3, 28.7, 27.6, 22.0, 10.5. HRMS (ESI): calcd for C$_{17}$H$_{25}$N$_3$O$_3$S (M+H)$^+$ = 352.1695, found 352.1698.

isopropyl 2-(4-methylpiperazine-1-carboxamido)-5,6-dihydro-4*H*-cyclopenta[*b*]thiophene-3-carboxylate (**11**)

Yield: 82%. ^{1}H NMR (400 MHz, CDCl$_3$) δ 10.85 (s, 1H), 5.14-5.20 (m, 1H), 3.59-3.61 (m, 4H), 2.81-2.88 (m, 4H), 2.48-2.51 (m, 4H), 2.35-2.38 (m, 5H), 1.35 (d, J = 7.2 Hz, 6H). ^{13}C NMR (101 MHz, CDCl$_3$) δ 166.1, 155.1, 152.6, 140.8, 130.0, 106.2, 67.5, 54.4, 45.9, 43.5, 30.3, 28.7, 27.6, 21.9. HRMS (ESI): calcd for C$_{17}$H$_{25}$N$_3$O$_3$S (M+H)$^+$ = 352.1695, found 352.1699.

2-(4-methylpiperazine-1-carboxamido)-5,6-dihydro-4*H*-cyclopenta[*b*]thiophene-3-carboxylic acid (**12**)

Yield: 78%. ^{1}H NMR (400 MHz, DMSO-d$_6$) δ 10.92 (s, 1H), 3.35-3.81 (m, 9H), 2.74-2.82 (m, 7H), 2.78-2.33 (m, 2H). ^{13}C NMR (101 MHz, DMSO-d$_6$) δ 167.7, 154.3, 152.3, 141.5, 130.0, 107.2, 51.9, 42.4, 40.9, 30.3, 28.8, 27.7. HRMS (ESI): calcd for C$_{14}$H$_{19}$N$_3$O$_3$S (M-H)$^-$ = 308.1069, found 308.1065.

methyl

2-(4-methylpiperazine-1-carboxamido)-4,5,6,7-tetrahydrobenzo[*b*]thiophene-3-carbox

ylate (**13**)

Yield: 92%. ^{1}H NMR (400 MHz, CDCl$_3$) δ 11.12 (s, 1H), 3.84 (s, 3H), 3.57-3.60 (m, 4H), 260-2.72 (m, 4H), 2.46-2.49 (m, 4H), 2.33 (s, 3H), 1.77-1.78 (m, 4H). ^{13}C NMR (101 MHz, CDCl$_3$) δ 167.8, 152.9, 151.7, 130.2, 125.0, 109.0, 54.4, 51.2, 45.9, 43.6, 26.2, 24.2, 22.9, 22.8. HRMS (ESI): calcd for C$_{16}$H$_{23}$N$_3$O$_3$S (M+H)$^+$ = 338.1538, found 338.1542.

methyl

2-(4-methylpiperazine-1-carboxamido)-5,6,7,8-tetrahydro-4*H*-cyclohepta[*b*]thiophene

-3-carboxylate (**14**)

Yield: 88%. ^{1}H NMR (400 MHz, CDCl$_3$) δ 11.08 (s, 1H), 3.85 (s, 3H), 3.56-3.58 (m, 4H), 2.98-2.99 (m, 2H), 2.67-2.68 (m, 2H), 2.45-2.48 (m, 4H), 2.33 (s, 3H), 1.81-1.83 (m, 2H), 1.61-1.64 (m, 4H). ^{13}C NMR (101 MHz, CDCl$_3$) δ 167.9, 153.0, 149.9, 135.7, 129.1, 110.3, 54.4, 51.3, 45.9, 43.6, 32.1, 28.4, 28.2, 27.7, 27.0. HRMS (ESI): calcd for C$_{15}$H$_{21}$N$_3$O$_3$S (M+H)$^+$ = 324.1382, found 324.1386.

methyl

6-methyl-2-(4-methylpiperazine-1-carboxamido)-4,5,6,7-tetrahydrobenzo[*b*]thiophen

e-3-carboxylate (**15**)

Yield: 87%. ^{1}H NMR (400 MHz, CDCl$_3$) δ 11.30 (d, *J* = 6.4 Hz, 1H), 4.19-4.23 (m, 2H), 3.83-3.88 (m, 5H), 3.57-3.60 (m, 2H), 2.85-2.94 (m, 6H), 2.64-2.69 (m, 2H),

2.21-2.23 (m, 1H), 1.82-1.88 (m, 2H), 133-1.36 (m, 1H), 1.05 (d, J = 6.4 Hz, 3H). ^{13}C NMR (101 MHz, DMSO-d_6) δ 166.8, 152.4, 150.0, 130.1, 124.8, 109.5, 52.0, 51.9, 42.3, 40.9, 32.1, 30.9, 29.1, 26.0, 21.6. HRMS (ESI): calcd for $C_{17}H_{25}N_3O_3S$ (M+H)$^+$ = 352.1695, found 352.1698.

methyl

2-(4-methylpiperazine-1-carboxamido)-6-pentyl-4,5,6,7-tetrahydrobenzo[b]thiophene

-3-carboxylate (**16**)

Yield: 80%. ^{1}H NMR (400 MHz, CDCl$_3$) δ 11.29 (s, 1H), 3.57-4.02 (m, 11H), 2.85-2.89 (m, 5H), 2.59-2.73 (m, 2H), 2.22-2.25 (m, 1H), 1.88-1.92 (m, 1H), 1.71 (s, 1H), 1.29-1.37 (m, 8H), 0.87-0.91 (m, 3H). ^{13}C NMR (101 MHz, DMSO-d_6) δ 166.8, 152.4, 150.3, 130.4, 124.9, 109.6, 52.1, 51.9, 43.5, 40.9, 35.8, 34.1, 31.9, 30.4, 29.0, 26.4, 26.0, 22.5, 14.3. HRMS (ESI): calcd for $C_{21}H_{33}N_3O_3S$ (M+H)$^+$ = 408.2321, found 408.2326.

ethyl

2-(4-methylpiperazine-1-carboxamido)-4,5,6,7-tetrahydrobenzo[b]thiophene-3-carbox

ylate (**17**)

Yield: 88%. ^{1}H NMR (400 MHz, CDCl$_3$) δ 11.16 (s, 1H), 4.32 (q, 2H), 3.59-3.61 (m, 4H), 2.62-2.76 (m, 4H), 2.49-2.51 (m, 4H), 2.35 (s, 3H), 1.77-1.81 (m, 4H), 1.39 (t, J_1 = 7.2 Hz, J_2 = 14.4 Hz, 3H). ^{13}C NMR (101 MHz, CDCl$_3$) δ 167.2, 152.9, 151.5, 130.2, 124.9, 109.1, 60.1, 54.4, 459, 43.5, 26.3, 24.1, 22.9, 22.8, 14.2. HRMS (ESI): calcd for $C_{17}H_{25}N_3O_3S$ (M+H)$^+$ = 352.1695, found 352.1699.

23

propyl

2-(4-methylpiperazine-1-carboxamido)-4,5,6,7-tetrahydrobenzo[*b*]thiophene-3-carbox

ylate (**18**)

Yield: 83%. ^{1}H NMR (400 MHz, CDCl$_3$) δ 11.17 (s, 1H), 4.20-4.23 (m, 2H), 3.56-3.58 (m, 4H), 2.62-2.75 (m, 4H), 2.45-2.48 (m, 4H), 2.33 (s, 3H), 1.74-1.80 (m, 6H), 1.02 (t, J_1 = 7.2 Hz, J_2 = 14.4 Hz, 3H). ^{13}C NMR (101 MHz, CDCl$_3$) δ 167.3, 152.8, 151.5, 130.1, 124.8, 109.0, 65.8, 54.4, 45.9, 43.6, 26.3, 24.1, 22.9, 22.8, 21.9, 10.6. HRMS (ESI): calcd for C$_{18}$H$_{27}$N$_3$O$_3$S (M+H)$^+$ = 366.1851, found 366.1856.

isopropyl

2-(4-ethylpiperazine-1-carboxamido)-5,6-dihydro-4*H*-cyclopenta[*b*]thiophene-3-carb

oxylate (**19**)

Yield: 82%. ^{1}H NMR (400 MHz, CDCl$_3$) δ 10.84 (s, 1H), 5.14-5.18 (m, 1H), 3.58-3.62 (m, 4H), 2.80-2.90 (m, 4H), 2.47-2.54 (m, 6H), 2.34-2.38 (m, 2H), 1.34 (d, J = 6.4 Hz, 6H), 1.11-1.14 (m, 3H). ^{13}C NMR (101 MHz, CDCl$_3$) δ 166.1, 155.2, 152.6, 140.8, 130.0, 1062, 67.5, 52.1, 52.0, 43.6, 30.3, 28.7, 27.6, 21.9, 11.7. HRMS (ESI): calcd for C$_{18}$H$_{27}$N$_3$O$_3$S (M+H)$^+$ = 366.1851, found 366.1855.

isopropyl

2-(4-phenylpiperazine-1-carboxamido)-5,6-dihydro-4*H*-cyclopenta[*b*]thiophene-3-car

boxylate (**20**)

Yield: 81%. ^{1}H NMR (400 MHz, CDCl$_3$) δ 10.94 (s, 1H), 7.28-7.33 (m, 3H),

6.95-7.00 (m, 2H), 5.17-5.20 (m, 1H), 3.76-3.77 (m, 4H), 3.28-3.31 (m, 4H), 2.83-2.90 (m, 4H), 2.37-2.40 (m, 2H), 1.37 (d, J = 6.0 Hz, 6H). ^{13}C NMR (101 MHz, CDCl$_3$) δ 166.3, 155.2, 152.8, 150.8, 141.0, 130.2, 129.2, 120.3, 116.4, 106.5, 67.7, 49.0, 43.6, 30.5, 28.8, 27.7, 22.1. HRMS (ESI): calcd for C$_{22}$H$_{27}$N$_3$O$_3$S (M+H)$^+$ = 414.1851, found 414.1856.

isopropyl

2-(4-methylpiperazine-1-carbothioamido)-5,6-dihydro-4*H*-cyclopenta[*b*]thiophene-3-

carboxylate (**21**)

Yield: 88%. ^{1}H NMR (400 MHz, CDCl$_3$) δ 12.13 (s, 1H), 5.16-5.22 (m, 1H), 4.09-4.12 (m, 4H), 2.91 (t, 2H), 2.84 (t, 2H), 2.65-2.67 (m, 4H), 2.42 (s, 3H), 2.37 (t, 2H), 1.36 (d, J = 6.4 Hz, 6H). ^{13}C NMR (101 MHz, CDCl$_3$) δ 175.8, 166.7, 155.6, 140.8, 131.4, 108.8, 68.1, 54.2, 47.4, 45.5, 30.5, 28.8, 27.6, 22.0. HRMS (ESI): calcd for C$_{17}$H$_{25}$N$_3$O$_2$S$_2$ (M+H)$^+$ = 368.1466, found 368.1468.

isopropyl

2-(4-phenylpiperazine-1-carbothioamido)-5,6-dihydro-4*H*-cyclopenta[*b*]thiophene-3-

carboxylate (**22**)

Yield: 80%. ^{1}H NMR (400 MHz, CDCl$_3$) δ 12.18 (s, 1H), 7.31-7.35 (m, 2H), 6.95-6.99 (m, 3H), 5.18-5.24 (m, 1H), 4.21-4.24 (m, 4H), 3.39-3.41 (m, 4H), 2.84-2.95 (m, 4H), 2.36-2.40 (m, 2H), 1.37 (d, J = 7.2 Hz, 6H). ^{13}C NMR (101 MHz, CDCl$_3$) δ 175.9, 166.8, 155.6, 150.2, 140.9, 131.5, 129.3, 120.2, 115.9, 108.9, 68.1, 48.4, 47.5, 30.5, 28.8, 27.7, 22.0. HRMS (ESI): calcd for C$_{22}$H$_{27}$N$_3$O$_2$S$_2$ (M+H)$^+$ = 430.1623, found 430.1627.

isopropyl

2-(piperazine-1-carbothioamido)-5,6-dihydro-4H-cyclopenta[b]thiophene-3-carboxyla

te (**23**)

Yield: 77%. ^{1}H NMR (400 MHz, CDCl$_3$) δ 12.07 (s, 1H), 5.17-5.21 (m, 1H), 4.29 (s,

1H), 3.98-4.02 (m, 2H), 2.82-3.02 (m, 7H), 2.59-2.68 (m, 2H), 2.17-2.40 (m, 3H),

1.36 (d, J = 5.6 Hz, 6H). ^{13}C NMR (101 MHz, CDCl$_3$) δ 175.6, 166.5, 155.7, 140.7,

131.1, 108.6, 68.0, 49.0, 45.6, 30.5, 28.8, 27.6, 22.0. HRMS (ESI): calcd for

C$_{16}$H$_{23}$N$_3$O$_2$S$_2$ (M+H)$^+$ = 354.1310, found 354.1315.

isopropyl

2-(4-acetylpiperazine-1-carbothioamido)-5,6-dihydro-4H-cyclopenta[b]thiophene-3-c

arboxylate (**24**)

Yield: 83%. ^{1}H NMR (400 MHz, CDCl$_3$) δ 12.14 (s, 1H), 5.14-5.20 (m, 1H),

3.99-4.16 (m, 4H), 3.66-3.83 (m, 4H), 2.81-2.92 (m, 4H), 2.34-2.38 (m, 2H), 2.14 (s,

3H), 1.35 (d, J = 6.0 Hz, 6H). ^{13}C NMR (101 MHz, CDCl$_3$) δ 175.6, 169.2, 166.5,

155.1, 140.8, 1313, 108.8, 68.1, 46.8, 46.8, 44.9, 40.1, 30.4, 28.7, 27.6, 21.9, 21.3.

HRMS (ESI): calcd for C$_{18}$H$_{25}$N$_3$O$_3$S$_2$ (M+H)$^+$ = 396.1416, found 396.1419.

ethyl

2-(4-methylpiperazine-1-carbothioamido)-4,5,6,7-tetrahydrobenzo[b]thiophene-3-car

boxylate (**25**)

Yield: 89%. ^{1}H NMR (400 MHz, CDCl$_3$) δ 12.44 (s, 1H), 4.34 (q, 2H), 4.04-4.05 (m, 4H), 2.77-2.78 (m, 2H), 2.55-2.65 (m, 6H), 2.37 (s, 3H), 1.79 (s, 4H), 1.40 (t, J_1 = 7.2 Hz, J_2 = 14.4 Hz, 3H). ^{13}C NMR (101 MHz, CDCl$_3$) δ 176.1, 167.7, 152.2, 130.2, 125.7, 111.4, 60.5, 54.3, 47.7, 45.6, 26.3, 24.2, 22.9, 22.9, 14.2. HRMS (ESI): calcd for C$_{17}$H$_{25}$N$_3$O$_2$S$_2$ (M+H)$^+$ = 368.1466, found 368.1469.

propyl

2-(4-methylpiperazine-1-carbothioamido)-4,5,6,7-tetrahydrobenzo[*b*]thiophene-3-car boxylate (**26**)

Yield: 84%. ^{1}H NMR (400 MHz, CDCl$_3$) δ 12.46 (s, 1H), 4.24 (t, J_1 = 6.4 Hz, J_2 = 12.8 Hz, 2H), 4.04-4.06 (m, 4H), 2.64-2.78 (m, 4H), 2.55-2.58 (m, 4H), 2.37 (s, 3H), 1.78-1.80 (m, 6H), 1.04 (t, J_1 = 7.2 Hz, J_2 = 14.4 Hz, 3H). ^{13}C NMR (101 MHz, CDCl$_3$) δ 175.9, 167.6, 152.1, 130.0, 125.3, 111.2, 66.2, 54.3, 47.6, 45.6, 26.2, 24.1, 22.9, 22.8, 21.9, 10.7. HRMS (ESI): calcd for C$_{18}$H$_{27}$N$_3$O$_2$S$_2$ (M+H)$^+$ = 382.1623, found 382.1627.

isopropyl

2-(4-methylpiperazine-1-carbothioamido)-4,5,6,7-tetrahydrobenzo[*b*]thiophene-3-car boxylate (**27**)

Yield: 83%. ^{1}H NMR (400 MHz, CDCl$_3$) δ 12.47 (s, 1H), 5.20-5.23 (m, 1H), 4.02-4.05 (m, 4H), 2.64-2.77 (m, 4H), 2.53-2.56 (m, 4H), 2.36 (s, 3H), 1.77-1.80 (m, 4H), 1.36 (d, J = 6.0 Hz, 6H). ^{13}C NMR (101 MHz, CDCl$_3$) δ 176.2, 167.2, 152.0,

130.3, 125.7, 111.8, 68.1, 54.4, 47.8, 45.7, 26.4, 24.2, 22.9, 22.0. HRMS (ESI): calcd

for $C_{18}H_{27}N_3O_2S_2$ $(M+H)^+$ = 382.1623, found 382.1628.

isopropyl

2-(4-methylpiperazine-1-carbothioamido)-5,6,7,8-tetrahydro-4*H*-cyclohepta[*b*]thioph

ene-3-carboxylate (**28**)

Yield: 80%. ^{1}H NMR (400 MHz, CDCl$_3$) δ 12.39 (s, 1H), 5.22-5.25 (m, 1H),

4.00-4.03 (m, 4H), 3.02-3.05 (m, 2H), 2.71-2.74 (m, 2H), 2.52-2.55 (m, 4H), 2.35 (s,

3H), 1.83-1.84 (m, 2H), 1.62-1.68 (m, 4H), 1.37 (d, *J* = 6.4 Hz, 6H). ^{13}C NMR (101

MHz, CDCl$_3$) δ 176.1, 167.3, 149.9, 135.8, 129.8, 113.1, 68.4, 54.3, 47.7, 45.6, 32.9,

28.4, 28.2, 27.7, 26.7, 21.9. HRMS (ESI): calcd for $C_{19}H_{29}N_3O_2S_2$ $(M+H)^+$ =

396.1779, found 396.1783.

4.2. Biology assays

4.2.1 QUANTI-Blue SEAP Assay.

HEK-Blue hTLR2 (or TLR3, TLR4) cells were cultured in 96-well plates (4×10^4

cells per well) of 200 μL DMEM (supplemented with 10% FBS, 10 ×

penicillin/streptomycin, and 10 × L-glutamine) at 37 °C for 24 hours before drug

treatment on the first day. In the next 24 hours of treatment, medium was removed

from the 96-well plate and substituted with 200 μL of DMEM containing indicated

concentrations of compounds, with/without different antibodies (0 to 10 μg/mL),

including anti-hTLR1–IgG, anti-hTLR2–IgA, or anti-hTLR6–IgA (InvivoGen) in the

antibody experiments. A sample buffer (50 μL) was collected and transferred from each well of the cell culture supernatants to a transparent 96-well plate (Thermo Scientific). Each well was treated with 50 μL of QUANTI-Blue (InvivoGen) buffer and incubated at 37 °C for 0.5-1 hour. Then measure the purple color by using a plate reader at an absorbance of 620 nm (A620).

4.2.2 ELISA Assay

THP-1 cells at a density of 2.5×10^5 cells/mL were differentiated by treatment with 100 nM PMA (Sigma) in RPMI cell culture medium, containing 10% FBS, 1% penicillin and streptomycin for 24 h at 37 °C in a 5% CO_2 humidified incubator. After that, cells were washed with PBS and cultured in fresh RPMI cell culture medium (containing 10% FBS, 1% pen/strep) for 24 h. Then, change the medium to RPMI only and treat with indicated concentration of compound for 4 hours. The cell culture supernatants were collected and froze at -80 °C until measurement. The level of cytokine TNF-α were determined using recombinant cytokine standards, cytokine-specific capture antibodies and detection antibodies according to the commercially available ELISA kit (BD Biosciences) with each sample for duplicate.

4.2.3 Western blotting analysis.

In the first day, 3 mL of HEK-Blue hTLR2 cells were seeded in 6-well plate (Thermo Scientific) at density of 1.5×10^6 per well in 3 mL DMEM (supplemented with 10% FBS, $10 \times$ penicillin/streptomycin, and $10 \times$ L-glutamine) and incubated for 24 hours.

In the second day, removed and replaced the medium with DMEM medium only to 3mL totally and treated the cells with different concentration of SMU-C13 and incubated for 24 hours. In the third day, the cells were harvested and lysed with 150 μL cell lysis buffers (PIPA mixed with PMSF at ratio of 50:1 before use, Boster). Cell lysates of equal amount were denatured, separated by sodium dodecyl sulfate polycrylamide gel electrophoresis (SDS-PAGE), and transferred to nitrocellulose membrane. Then use PBS (containing 5% nonfat milk) to block the membrane for 2 h , and then incubated with the primary antibody of TLR2 overnight at 4 °C, followed with incubating by a horseradish peroxidase conjugated secondary antibody. The immunoblots were visualized by enhanced exposure machine. During the operation, the following primary and secondary antibodies were employed: mouse-GAPDH (1:2000, Solarbio, M1000110), rabbit-TLR2 (1:2000, Cell Signaling, 12276), goat-anti-mouse-GAPDH-HRP (1:2500, Boster, BA1050) and goat-anti-rabbit-TLR2-HRP (1:1000, Solarbio, SE134).

4.2.4 Cell viability.

HEK-Blue hTLR2 cells were cultured in 96-well plates (4×10^4 cells per well) of 200 μL DMEM (supplemented with 10% FBS, $10 \times$ penicillin/streptomycin, and $10 \times$ L-glutamine) at 37 °C for 24 hours before drug treatment. After incubation, indicated concentration compounds were add to 200 μL DMEM totally and incubated at 37$^\text{o}$C for another 24h. After 100 μL supernatant was removed, 10 μL Cell counting kit-8 (CCK-8) (Bimake, B34304, USA) was added to each well of above 96-well plate and

incubated at 37°C for 1-4h until it turned into orange. Then the plate was measured at an absorbance of 450 nm through a plate reader.

4.2.5 Computer simulation.

Compound SMU-C13 was docked into the TLR1 and TLR2 binding domain (PDB: 2Z7X) using Glide 7.4. The molecule is created, as appropriate, with multiple protonation and tautomeric states. The TLR1/2 conformations were prepared using standard Glide protocols. This includes addition of hydrogens, restrained energy-minimizations of the protein structure with the Optimized Potentials for Liquid Simulations-All Atom (OPLS-AA) force field, and finally setting up the Glide grids using the Protein and Ligand Preparation Module [17].

Appendix A. Supplementary data

Supporting Information Available: Supplementary data for the NMR spectra associated with this article can be found in the online version at http://

References

1. T. Kawai, S. Akira, Toll-like receptors and their crosstalk with other innate receptors in infection and immunity, Immunity 34 (5) (2011) 637-650.

2. A.A. Abdul-Sater, M.I. Edilova, D.L. Clouthier, A. Mbanwi, E. Kremmer, T.H. Watts, The signaling adaptor TRAF1 negatively regulates Toll-like receptor signaling and this underlies its role in rheumatic disease, Nat Immunol. 18 (2017) 26-35.

3. S. K. Ippagunta, J. A. Pollock, N. Sharma, W. Lin, T. Chen, K. Tawaratsumida, A. A. High, J. Min, Y. Chen, R. K. Guy, V. Redecke, J. A. Katzenellenbogen, H. Häcker, Identification of Toll-like receptor signaling inhibitors based on selective activation of hierarchically acting signaling proteins, Sci Signal. 11 (2018) eaaq1077.

4. T. Kawai, S. Akira, The role of pattern-recognition receptors in innate immunity: update on Toll-like receptors, Nat Immunol. 11 (2010) 373-384.

5. F. Leulier, B. Lemaitre, Toll-like receptors - taking an evolutionary approach, Nat Rev Genet. 9 (2008) 165-178.

6. L.A. O'Neill, D. Golenbock, A.G. Bowie, The history of Toll-like receptors -redefining innate immunity, Nat Rev Immunol. 13 (2013) 453-460.

7. L. Israel, Y. Wang, K. Bulek, E. Della Mina, Z. Zhang, V. Pedergnana, M. Chrabieh, N. A. Lemmens, V. Sancho-Shimizu, M. Descatoire, T. Lasseau, E. Israelsson, L. Lorenzo, L. Yun, A. Belkadi, A. Moran, L. E. Weisman, F. Vandenesch, F. Batteux, S. Weller, M. Levin, J. Herberg, A. Abhyankar, C. Prando,

Y. Itan, W. J. B. van Wamel, C. Picard, L. Abel, D. Chaussabel, X. Li, B. Beutler, P. D. Arkwright, J.-L. Casanova, A. Puel, Human adaptive immunity rescues an inborn error of innate immunity, Cell 168 (2017) 789-800.

8. M. Mellett, P. Atzei, R. Bergin, A. Horgan, T. Floss, W. Wurst, J.J. Callanan, P.N. Moynagh, Orphan receptor IL-17RD regulates Toll-like receptor signalling via SEFIR/TIR interactions, Nat Commun. 6 (2015) 6669.

9. M.S. Jin, S.E. Kim, J.Y. Heo, M.E. Lee, H.M. Kim, S.G. Paik, H. Lee, J.O. Lee, Crystal structure of the TLR1-TLR2 heterodimer induced by binding of a tri-acylated lipopeptide, Cell 130 (2007) 1071-1082.

10. M.A. Ciorba, T.E. Riehl, M.S. Rao, C. Moon, X. Ee, G.M. Nava, M.R. Walker, J.M. Marinshaw, T.S. Stappenbeck, W.F. Stenson, Lactobacillus probiotic protects intestinal epithelium from radiation injury in a TLR-2/cyclo-oxygenase-2-dependent manner. Gut 61 (2012) 829-838.

11. S.A. Freeman, V. Jaumouillé, K. Choi, B.E. Hsu, H.S. Wong, L. Abraham, M.L. Graves, D. Coombs, C.D. Roskelley, R. Das, S. Grinstein, M.R. Gold, Toll-like receptor ligands sensitize B-cell receptor signalling by reducing actin-dependent spatial confinement of the receptor, Nat Commun. 6 (2015) 6168

12. H. Lu, Y. Yang, E. Gad, C.A. Wenner, A. Chang, E.R. Larson, Y. Dang, M. Martzen, L.J. Standish, Disis, M. L., Polysaccharide krestin is a novel TLR2 agonist that mediates inhibition of tumor growth via stimulation of CD8 T cells and NK cells, Clin Cancer Res. 17 (2011) 67-76.

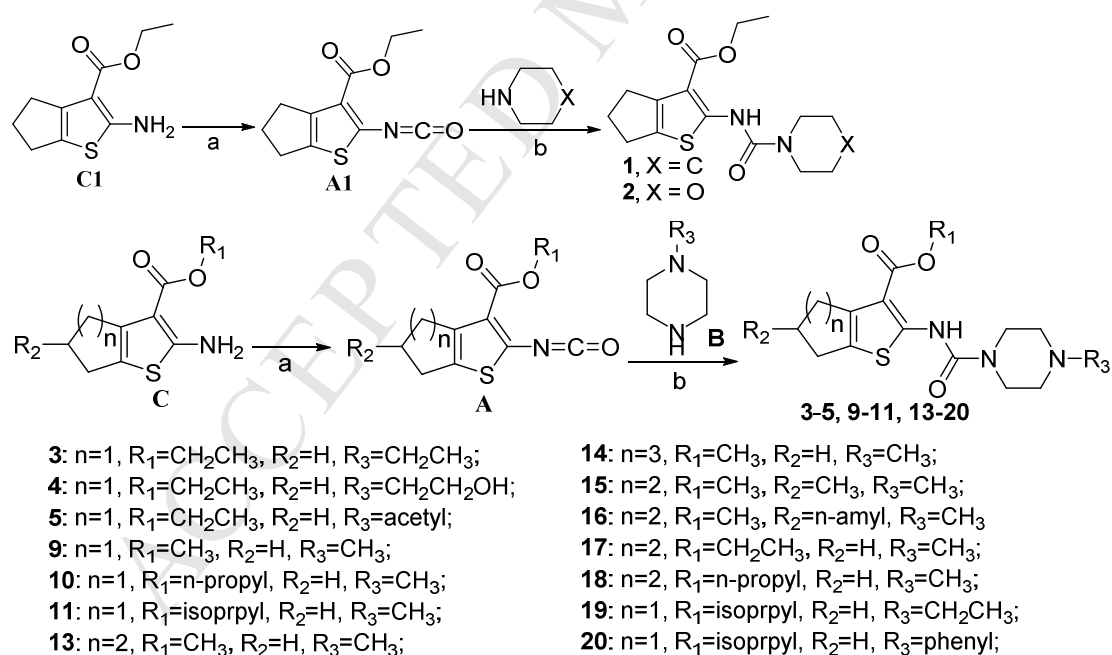13. Y. Zhang, F. Luo, A. Li, J. Qian, Z. Yao, X. Feng, Y. Chu, Systemic injection of

TLR1/2 agonist improves adoptive antigen-specific T cell therapy in glioma-bearing mice, Clinical Immunology, 154 (2014) 26-36.

14. S.K. Lee, J.Y. Chwee, C.A. Ma, B.N. Le, C.W. Huang, S. Gasser, Synergistic anticancer effects of Pam3CSK4 and Ara-C on B-cell lymphoma cells, Clinical Cancer Research, 20 (2014) 3485-3495.

15. Y. Wang, L. Su, M.D. Morin, B.T. Jones, Y. Mifune, H. Shi, K.-w. Wang, X. Zhan, A. Liu, J. Wang, X. Li, M. Tang, S. Ludwig, S. Hildebrand, K. Zhou, D.J. Siegwart, E.M.Y. Moresco, H. Zhang, D.L. Boger, B. Beutler, Adjuvant effect of the novel TLR1/TLR2 agonist Diprovocim synergizes with anti–PD-L1 to eliminate melanoma in mice, P Nati Acad Sci USA. 115 (2018) E8698-E8706.

16. M.D. Morin, Y. Wang, B.T. Jones, Y. Mifune, L. Su, H. Shi, E.M.Y. Moresco, H. Zhang, B. Beutler, D.L. Boger, Diprovocims: A New and Exceptionally Potent Class of Toll-like Receptor Agonists, J Am Chem Soc. 140 (2018) 14440-14454.

17. K. Cheng, X. Wang, H. Yin, Small-Molecule Inhibitors of the TLR3/dsRNA Complex, J Am Chem Soc. 133 (2011) 3764-3767.

18. X. Wang, C. Smith, H. Yin, Targeting Toll-like Receptors with Small Molecule Agents, Chem Soc Rev, 42 (2013) 4859-4866.

19. K. Cheng, X. Wang, S. Zhang, H. Yin, Discovery of small molecule inhibitors of the TLR1-TLR2 complex, Angew Chem Int Ed. 51 (2012) 12246-12249.

20. K. Cheng, M. Gao, J.I. Godfroy, P.N. Brown, N. Kastelowitz, H. Yin, Specific activation of the TLR1-TLR2 heterodimer by small-molecule agonists, Sci Adv. 1 (2015) e1400139.

21. Z. Chen, X. Cen, J. Yang, X. Tang, K. Cui, K. Cheng, Structure-based discovery of a specific TLR1-TLR2 small molecule agonist from the ZINC drug library database, Chem commun. 54 (2018) 11411-11414.

22. K. Gewald, E. Schinke, and H. Bottcher, 2-amino-thiophene aus methylenaktiven nitrilen, carbonylverbindugen und schwefel, Chemische Berichte, 99 (1966) 94-100.

23. H. Kai, Y. Morioka, Y. Koriyama *et al*., 2-Arylimino-5,6-dihydro-4H-1,3-thiazines as a new class of cannabinoid receptor agonists. Part 3: Synthesis and activity of isosteric analogs. Bioorg Med Chem Lett. 18(2008) 6444-6447.
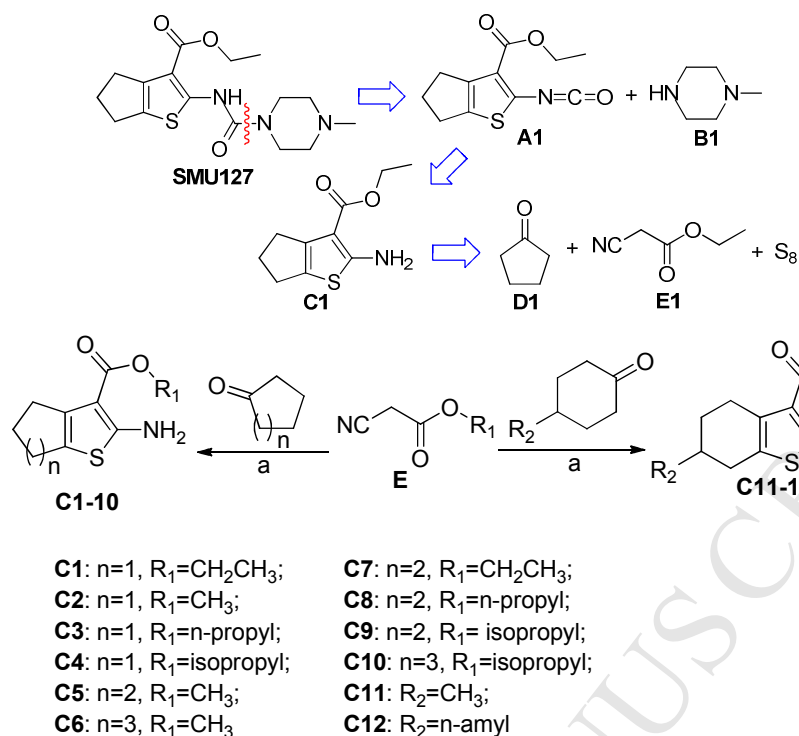
Scheme 1. Retrosynthesis of the lead compound and synthesis of intermediate C.
Reagents and conditions: (a) S_8, diethylamine, methanol/ethanol, ultrasonic, rt.

3: n=1, R_1=CH$_2$CH$_3$, R_2=H, R_3=CH$_2$CH$_3$;
4: n=1, R_1=CH$_2$CH$_3$, R_2=H, R_3=CH$_2$CH$_2$OH;
5: n=1, R_1=CH$_2$CH$_3$, R_2=H, R_3=acetyl;
9: n=1, R_1=CH$_3$, R_2=H, R_3=CH$_3$;
10: n=1, R_1=n-propyl, R_2=H, R_3=CH$_3$;
11: n=1, R_1=isoprpyl, R_2=H, R_3=CH$_3$;
13: n=2, R_1=CH$_3$, R_2=H, R_3=CH$_3$;

14: n=3, R_1=CH$_3$, R_2=H, R_3=CH$_3$;
15: n=2, R_1=CH$_3$, R_2=CH$_3$, R_3=CH$_3$;
16: n=2, R_1=CH$_3$, R_2=n-amyl, R_3=CH$_3$
17: n=2, R_1=CH$_2$CH$_3$, R_2=H, R_3=CH$_3$;
18: n=2, R_1=n-propyl, R_2=H, R_3=CH$_3$;
19: n=1, R_1=isoprpyl, R_2=H, R_3=CH$_2$CH$_3$;
20: n=1, R_1=isoprpyl, R_2=H, R_3=phenyl;

Scheme 2. Synthesis of urea compounds. Reagents and conditions: (a) triphosgene, dimethyl carbonate, 90°C, 8h; (b) dimethyl carbonate, rt.

36
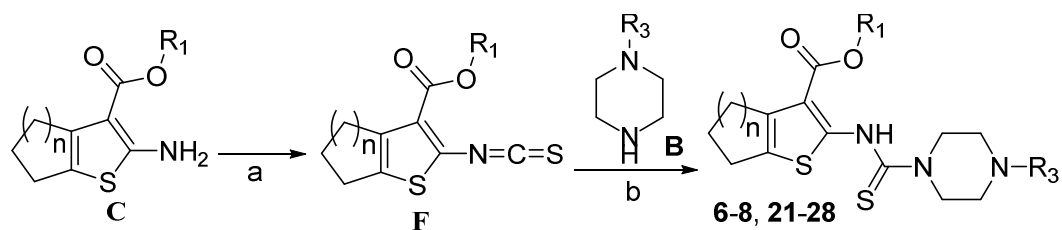
6: n=1, R$_1$=CH$_2$CH$_3$, R$_3$=CH$_3$;
7: n=1, R$_1$=CH$_2$CH$_3$, R$_3$=acetyl;
8: n=1, R$_1$=CH$_2$CH$_3$, R$_3$=phenyl;
21: n=1, R$_1$=isopropyl, R$_3$=CH$_3$;
22: n=1, R$_1$=isopropyl, R$_3$=phenyl;
23: n=1, R$_1$=isopropyl, R$_3$=H;

24: n=1, R$_1$=isopropyl, R$_3$=acetyl;
25: n=2, R$_1$=CH$_2$CH$_3$, R$_3$=CH$_3$;
26: n=2, R$_1$=n-propyl, R$_3$=CH$_3$;
27: n=2, R$_1$=isopropyl, R$_3$=CH$_3$
28: n=3, R$_1$=isopropyl, R$_3$=CH$_3$;
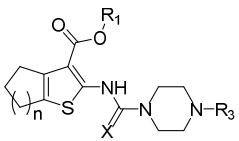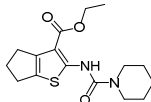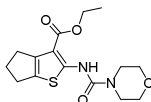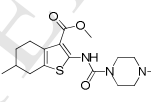
Scheme 3. Synthesis of thiourea compounds. Reagents and conditions: (a) thiophosgen, triethylamine, dichloromethane, 0°C; (b) dichloromethane, rt.

Table 1. Structure-activity relation analysis in HEK-Blue hTLR2 cells

Compounds	n	X	R_1	R_3	$EC_{50}/\mu M$[a]
SMU127	1	O	CH_2CH_3	CH_3	0.56±0.01
1					NA[b]
2					NA
3	1	O	CH_2CH_3	CH_2CH_3	8.55±3.46
4	1	O	CH_2CH_3	CH_2CH_2OH	NA
5	1	O	CH_2CH_3	$COCH_3$	NA
6	1	S	CH_2CH_3	CH_3	3.46±0.22
7	1	S	CH_2CH_3	$COCH_3$	NA
8	1	S	CH_2CH_3	phenyl	NA
9	1	O	CH_3	CH_3	0.45±0.03
10	1	O	$CH_2CH_2CH_3$	CH_3	14.16±2.81
11	1	O	$CH(CH_3)_2$	CH_3	4.59±0.49
12	1	O	H	CH_3	NA
13(SMU-C13)	2	O	CH_3	CH_3	0.16±0.01
14	3	O	CH_3	CH_3	1.33±0.02
15					11.82±1.92
16					NA
17	2	O	CH_2CH_3	CH_3	0.35±0.01
18	2	O	$CH_2CH_2CH_3$	CH_3	6.63±1.25
19	1	O	$CH(CH_3)_2$	CH_2CH_3	NA
20	1	O	$CH(CH_3)_2$	phenyl	NA
21	1	S	$CH(CH_3)_2$	CH_3	16.38±4.01
22	1	S	$CH(CH_3)_2$	phenyl	NA
23	1	S	$CH(CH_3)_2$	H	NA
24	1	S	$CH(CH_3)_2$	$COCH_3$	NA
25	2	S	CH_2CH_3	CH_3	6.43±0.41
26	2	S	$CH_2CH_2CH_3$	CH_3	NA
27	2	S	$CH(CH_3)_2$	CH_3	45.24±24.29
28	3	S	$CH(CH_3)_2$	CH_3	NA

[a] The numbers of EC_{50} are determined from at least three independent repeats.

[b] NA means no activity at the tested concentrations up to 200 µM.
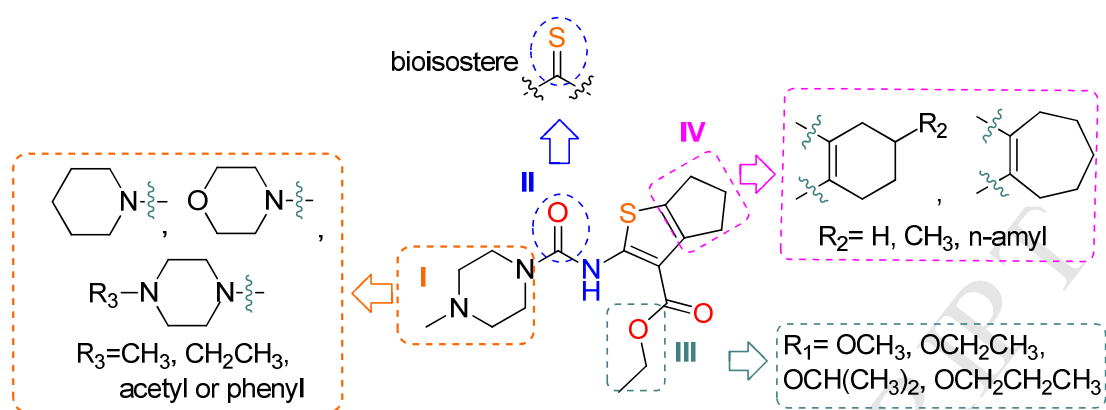
Figure 1. Structure of lead compound ZINC6662436 (SMU127) and areas of modification (I, II, III, IV).
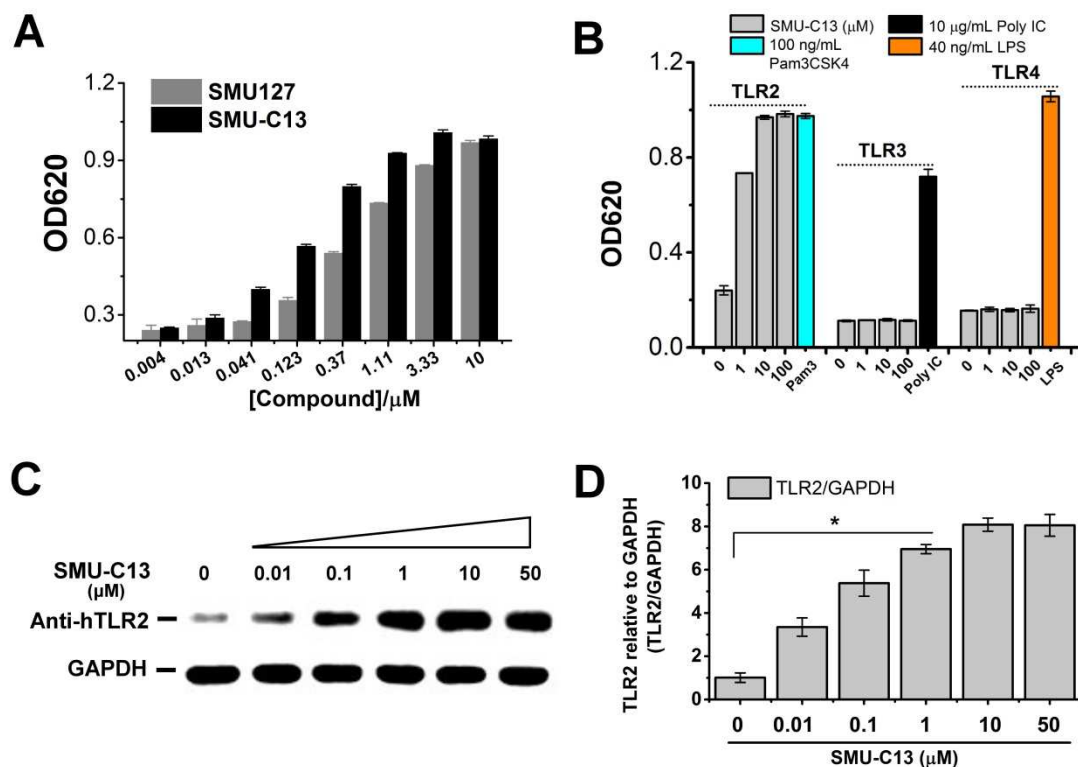
Figure 2. SMU-C13 is a specific agonist of TLR2. (A) Comparison of SMU-C13 and SMU127 activated secreted alkaline phosphatase (SEAP) signals in HEK-Blue hTLR2 cells. HEK-Blue hTLR2 cells were incubated with SMU127 or SMU-C13 for 24 hours, and the activation was measured by Quanti-Blue in the culture supernatants at OD620. (B) HEK-Blue Human TLR2, TLR3 and TLR4 cells were incubated with SMU-C13 (0 to 100 μM) with the control of TLR-specific agonists separately for 24 hours, and activation was evaluated by the optical density at 620nm. Agonist: TLR2, Pam3CSK4 (100 ng/mL); TLR3, poly IC (10 μg/mL) and TLR4, LPS (40 ng/mL). (C) SMU-C13 promoted the TLR2 protein expression in HEK-Blue hTLR2 cells. Cells were treated with SMU-C13 (0-50 μM) for 24 h, and the cell lysates were detected using Western blot and anti-TLR2 antibody. GAPDH served as the cell lysates input control. Data presented are mean ± SD and the figures shown are representative of three independent experiments. * P< 0.01.
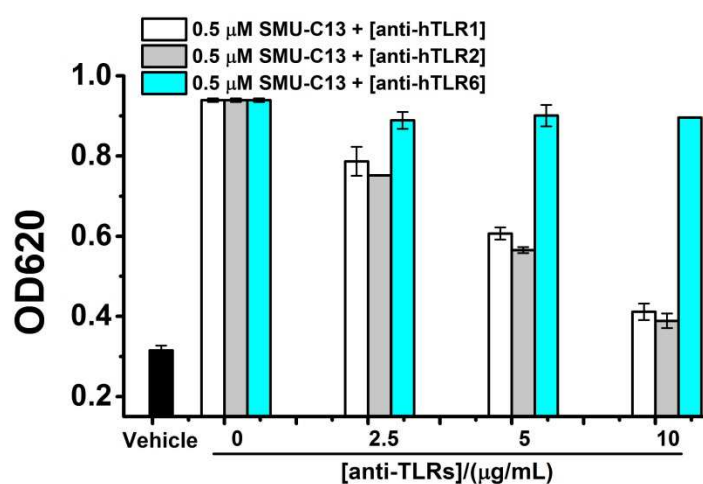
Figure 3. SMU-C13 is a specific agonist of TLR1/2, not TLR2/6. HEK-Blue hTLR2 cells were treated with 0.5µM SMU-C13 and antibodies of anti-hTLR1, anti-hTLR2, or anti-hTLR6 (0-10 μg/mL) for 24 hours, and the inhibition was measured by Quanti-Blue in the culture supernatants at OD620. Anti-hTLR1-IgG and anti-hTLR2-IgA antibodies can inhibit SMU-C13-triggered SEAP signaling on a dose-dependently manner, whereas anti-hTLR6-IgG has no influence to the SEAP signalling. Data presented are mean ± SD and the figures shown are representative of three independent experiments.
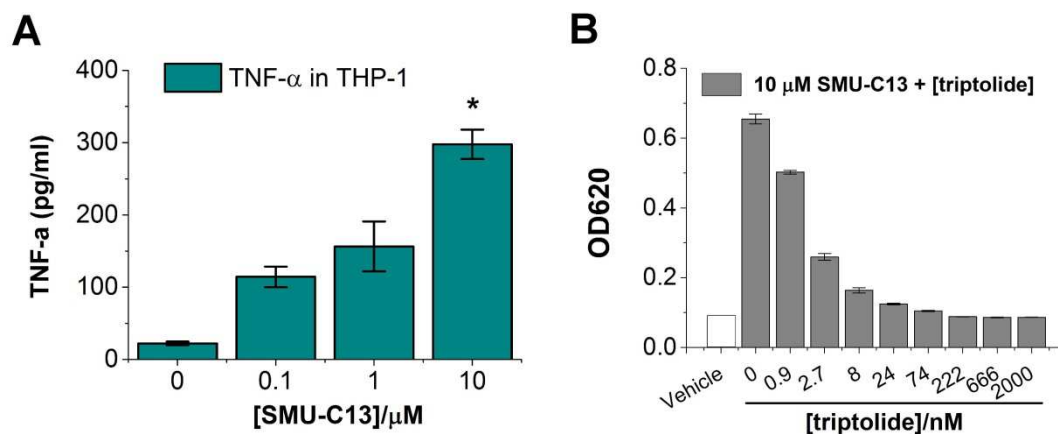
Figure 4. SMU-C13 induces TNFα production and SEAP secretion. (A) The TNF-α in the supernatants of human THP-1 cells after treatment with SMU-C13 for 4 h. (B) The SEAP expression after treat with SMU-C13 and with/without the classic NF-κB inhibitor triptolide. Data presented are mean ± SD and the figures shown are representative of three independent experiments. * P< 0.01.
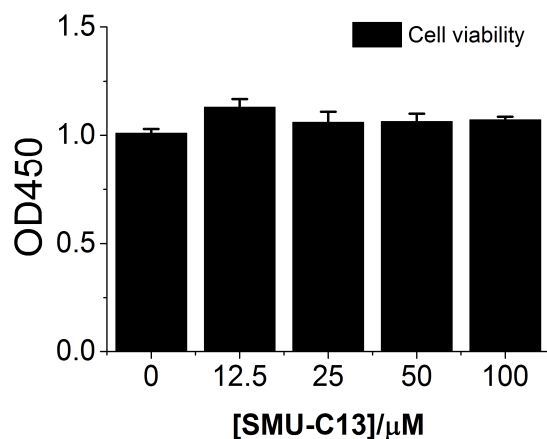
Figure 5. Cytotoxicity of SMU-C13 by CCK8 colorimetric method. HEK-Blue hTLR2 cells were cultured in DMEM at 37 °C for 24 hours before drug treatment. Indicated concentration compounds were added and incubated at 37°C for another 24h. The cell viability was detected through Cell counting kit-8 (CCK-8) at OD450. Data presented are mean ± SD and the figures shown are representative of three independent experiments.
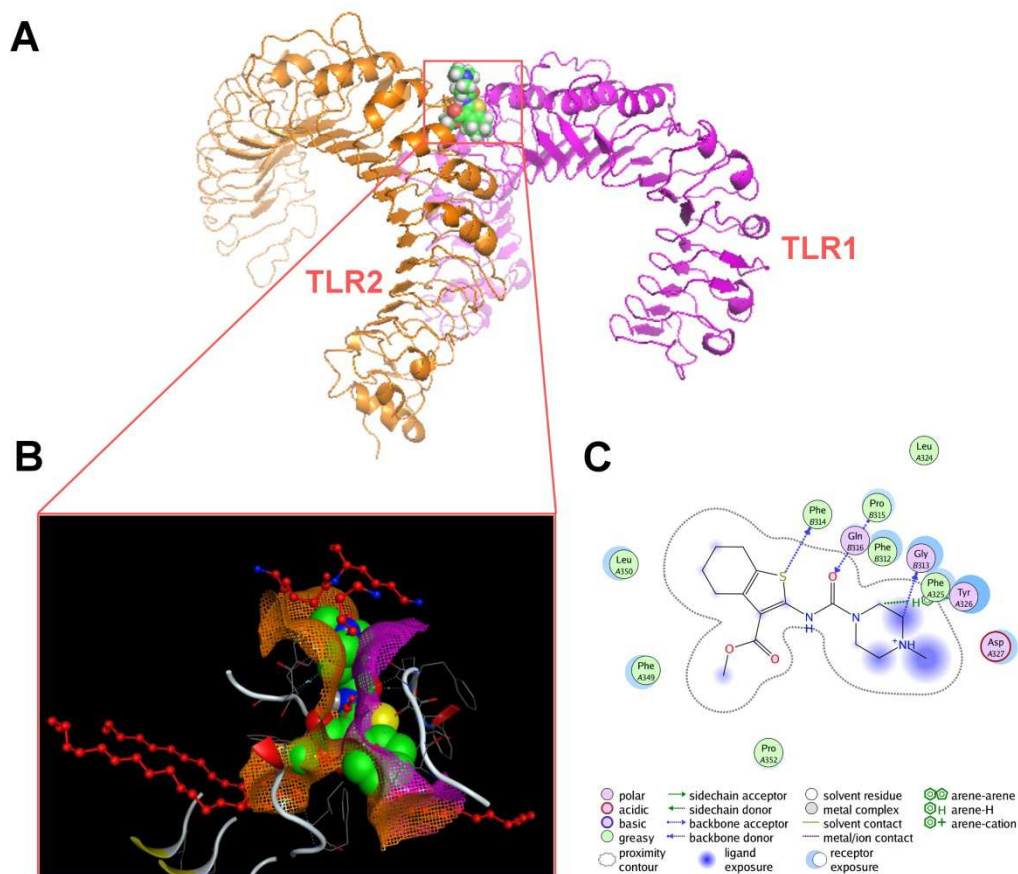
Figure 6. Low-energy binding conformations of SMU-C13 (green) and Pam3CSK4 (red) bound to the TLR1–TLR2 interface (PDB 2Z7X) as generated by virtual ligand docking. (A) Molecular docking of compound SMU-C13 (green) in the Pam3CSK4 binding pocket of human TLR1/2 complex (PDB 3FXI). (B) Overlay of binding geometry between compound SMU-C13 (green) and Pam3CSK4 (red line) with TLR1 (purple) and TLR2 (yellow). (C) The interaction between SMU-C13, and TLR1 (Chain B)/TLR2 (Chian A).

Highlights for this paper

- A series of novel N-aryl-N'-(thiophen-2-yl)thiourea analogues were generated to investigate their TLR2 activation with compound SMU-C13 optimized.
- SMU-C13 specificity actives TLR1/2, not TLR2/6.
- SMU-C13 provides a novel molecule probe for potential therapeutic applications, including vaccine adjuvants and tumor immunity therapies.